Calcified microbial reefs in Cambrian Series 2, North China Platform: Implications for the evolution of Cambrian calcified microbes

Jeong-Hyun Lee [a], Hyun Suk Lee [b], Jitao Chen [c], Jusun Woo [d], S.K. Chough [a],*

[a] School of Earth and Environmental Sciences, Seoul National University, Seoul 151-747, Republic of Korea
[b] Korea Institute of Geoscience and Mineral Resources, Daejeon 305-350, Republic of Korea
[c] Nanjing Institute of Geology and Palaeontology, Chinese Academy of Sciences, Nanjing 210008, China
[d] Division of Polar Earth-System Sciences, Korea Polar Research Institute, Incheon 406-840, Republic of Korea

ABSTRACT

This study focuses on the microbial reefs of the Zhushadong Formation (Cambrian Series 2) in Shandong Province, China in order to understand the evolution of calcified microbes in the North China Platform during the Cambrian Series 2 and 3. The microbial reefs occur in a thin unit, ca. 3 m thick, over an area of 1 km². They consist of three types of thrombolite based on their mesostructures: rimmed, grainstone-patch, and dendritic. The thrombolites mainly occur in various coarse-grained carbonate facies, including crudely stratified oolitic grainstone, stromatolitic grainstone, and disorganized limestone conglomerate. Calcified microbes in the thrombolites include *Epiphyton*, *Kordephyton*, a tubiform microbe, *Bija*, *Tarthinia*, *Renalcis*, *Amgaina*, and *Razumovskia*. The Zhushadong thrombolites were formed within a grainstone shoal, and experienced repeated burial and exposure. The rimmed thrombolite and grainstone-patch thrombolite experienced abundant input of carbonate grains (forming grainstone patches). In contrast, the dendritic thrombolite formed solely by calcification of microbes that mainly include *Epiphyton*, *Tarthinia*, and the tubiform microbe. The outer crusts of the rimmed thrombolite were formed by *Amgaina*, under high energy conditions.
The diverse calcified microbes of the Zhushadong Formation form the earliest assemblage of their type in the North China Platform. Their descendants, mostly *Epiphyton*, subsequently thrived, forming a ca. 180 m thick microbialite–oolite-dominated succession during the Cambrian Series 3 (Zhangxia Formation). Although the reefs in the Zhushadong Formation are much smaller than those of the overlying Zhangxia Formation, their calcified microbes are more diverse. This most likely reflects changes in depositional environments (e.g., abundant siliciclastic input and tidal effects vs. those of a stable carbonate platform), and/or global changes within reef environments (e.g., end-Cambrian Series 2 extinction of archaeocyaths and calcified microbes). A decrease in diversity of calcified microbes in the North China Platform, where archaeocyaths were absent, may help to account for evolutionary trends in calcified microbes that occurred independently of archaeocyath influence.

© 2014 Elsevier B.V. All rights reserved.

1. Introduction

Calcified microbes firstly appeared in the Precambrian and diversified greatly from the base of the Cambrian (Turner et al., 1993; Zhuravlev, 1996; Riding, 2001; Kah and Riding, 2007). During the early Cambrian (Terreneuvian and Series 2), calcified microbes formed reefs together with archaeocyaths in various localities including Siberia, Laurentia, North Africa, South China, Australia, Europe, and Antarctica (Rowland and Gangloff, 1988; Rowland and Shapiro, 2002; Gandin and Debrenne, 2010; and references therein). Although the diversity of calcified microbes decreased during the late Cambrian Series 2 along with the extinction of archaeocyaths (end-Cambrian Series 2 extinction event), microbes still constructed reefs during the Cambrian

Series 3 without reef-building metazoans (Zhuravlev, 1996; Zhuravlev and Wood, 1996; Pratt et al., 2001; Riding, 2001).

The end-Cambrian Series 2 extinction event was most likely caused by global environmental change such as anoxic oceanic conditions (Sinsk Event) and global regression (Hawke Bay Event) (Zhuravlev and Wood, 1996). These global events are thought to have resulted in modification of the calcified microbial community. For example, Zhuravlev (1996) suggested that loss of the ecological niche created by framework-building archaeocyaths, and homogenization of microbial communities due to the extinction of tiny grazers, could have caused the decrease in calcified microbe diversity. However, just how these mechanisms and global events reduced the diversity of calcified microbes has not been studied in detail.

In order to examine the relationships between the end-Cambrian Series 2 extinction event and decrease in the diversity of calcified microbes, this study focused on the Cambrian Series 2 microbial reefs

* Corresponding author.
  E-mail addresses: leejh85@snu.ac.kr (J.-H. Lee), sedlab@snu.ac.kr (S.K. Chough).

in the North China Platform, where a variety of microbial reefs flourished and formed extensive deposits during the Cambrian Series 3 (Woo et al., 2008; Woo and Chough, 2010; Howell et al., 2011). New discoveries of calcified microbes in the Cambrian Series 2 deposits, and comparison with those of the Cambrian Series 3, help to clarify the evolutionary history of calcified microbes on the North China Platform. Furthermore, the absence of archaeocyaths from the North China Platform (Chough et al., 2010; Gandin and Debrenne, 2010) could provide a unique opportunity for elucidating the direct effects of the environmental changes that are suggested to have caused end-Cambrian Series 2 calcified microbe extinctions, independently of archaeocyath extinction.

2. Geological setting

The North China Platform is a typical epeiric platform that existed throughout the Cambrian Series 2–Middle Ordovician (Meng et al., 1997; Kwon et al., 2006). The platform formed on a stable craton, the Sino-Korean Block, which was located near the margin of Gondwana during the Early Paleozoic (McKenzie et al., 2011). Paleomagnetic analyses suggest that the Sino-Korean Block was situated near the paleoequator during the Cambrian (Zhao et al., 1992; Huang et al., 2000; Yang et al., 2002). A 1800 m-thick mixed siliciclastic–carbonate succession was deposited in the North China Platform (Meng et al., 1997). In the central part of the North China Platform (Shandong Province, China), the carbonate-dominated Zhushadong Formation (10 to 50 m thick) unconformably overlies the Precambrian basement (Meng et al., 1997; Chough et al., 2010) (Fig. 1A). This formation passes laterally into the siliciclastic Liguan Formation (37 m thick) in eastern-most Shandong (Fig. 1B). Various limestones and dolostones including laminated/homogeneous dolo-mudstone, bioturbated dolo-wackestone, cross-stratified oolitic grainstone, limestone conglomerate, microbial laminites, and stromatolites occur in the Zhushadong Formation (Fig. 2). This assemblage of deposits represents carbonate dominated environments such as peritidal flats and ooid shoals, reflecting uneven topography and local variations in the carbonate factory (Lee and Chough, 2011). The Zhushadong Formation was deposited during the upper Tsanglangpuan Stage (*Megapalaeolenus* Zone), which can be correlated with informal Stage 3 of the Cambrian Series 2 (Geyer and Shergold, 2000; Peng et al., 2012).

3. Methods

The study area (Sunmayu section) is located in the southeastern part of Shandong Province (Fig. 1A). The Zhushadong Formation in this area is up to 50 m thick, and unconformably overlies Precambrian granitic gneiss (Fig. 2A). Thrombolites, containing clotted mesostructures (Aitken, 1967; Shapiro, 2000), mainly occur in a 3 m thick interval that occurs 31 m above the basement, and were examined in two sections (Sections 1 and 2), about 1.1 km apart (Fig. 2). Within Section 1, three sub-sections, 20 to 30 m apart, were selected to describe the lateral variations (Sections 1-1, 1-2, and 1-3). These sections were measured at a 1:50 scale (Fig. 2B, C). Sketches and line drawings of the thrombolites were made in the field, and slabs and thin sections were prepared in the laboratory to identify meso- and microscale fabrics.

4. Microbial reefs in the Zhushadong Formation

4.1. Macro- and mesoscale characteristics

Several types of dm- to m-scale thrombolite occur in the coarse-grained carbonate facies, including crudely stratified oolitic grainstone, stromatolitic grainstone, and disorganized limestone conglomerate (Fig. 2). Three types of thrombolite are recognized based on their mesostructures (cf., Shapiro, 2000; Chen and Lee, 2014): rimmed, grainstone-patch, and dendritic thrombolites (Table 1). Thrombolites are described here as microbial reefs, following the reef definition of Wood (1999): "a discrete carbonate structure formed by in-situ or bound organic components that develops topographic relief upon the sea floor".
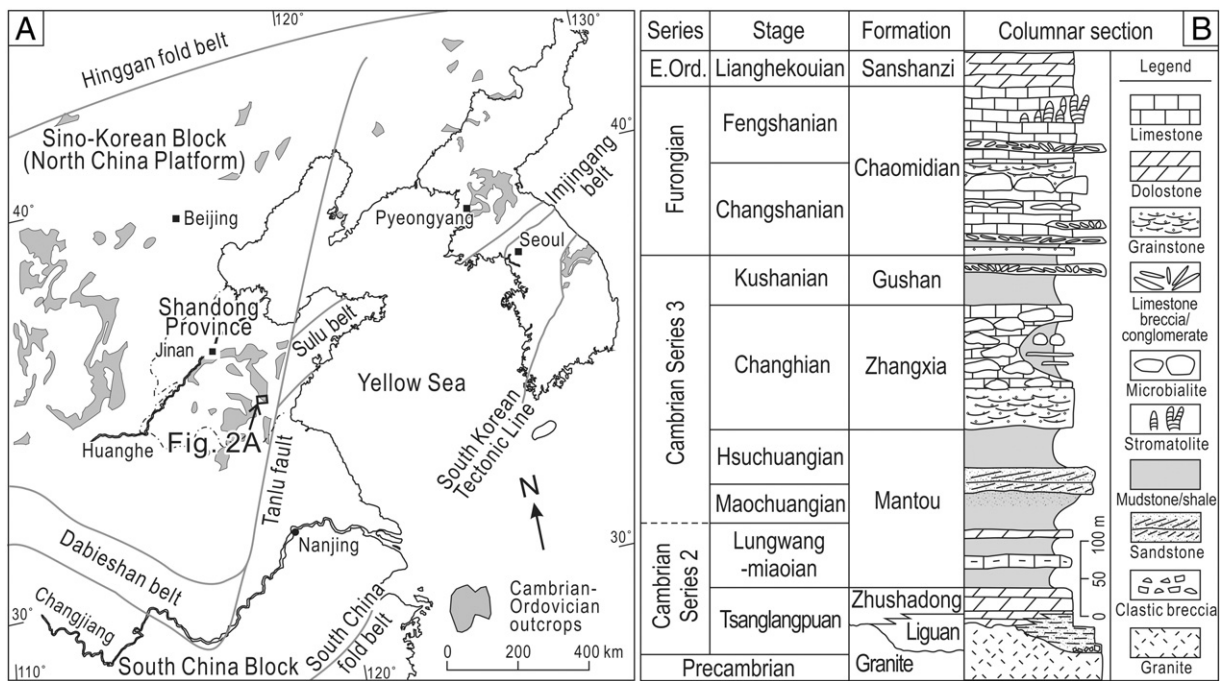
Fig. 1. Geological setting of the study area. (A) Cambrian–Ordovician outcrops in the North China Platform. Study area is marked with an arrow. (B) Summary of the Cambrian succession in Shandong Province, China.
Modified after Chough et al. (2010).
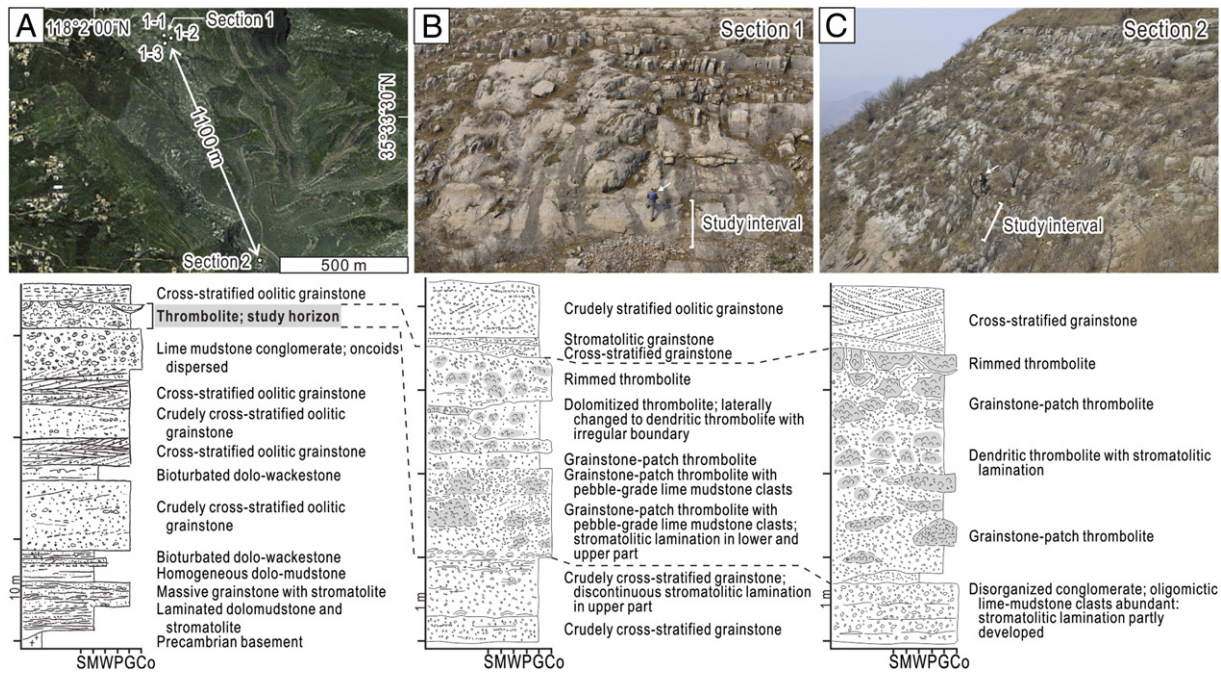
Fig. 2. (A) Satellite photograph (modified from Google Earth) and sedimentary log of the lower–middle part of the Zhushadong Formation in the Sunmayu section. Section 1 (35°33′39″N, 118°2′12″E); Section 2 (35°33′10″N, 118°2′27″E). Thrombolite-bearing horizon is marked in gray. (B) Outcrop photographs and sedimentary log of Section 1. Arrow indicates geologist for scale. (C) Outcrop photographs and sedimentary log of Section 2.

4.1.1. Rimmed thrombolite

4.1.1.1. Description. The rimmed thrombolites display a crudely laminated rim (or crust) and a thrombolitic core (Fig. 3A). The rim consists of two zones. The outer zone is 1 to 5 cm thick, consisting of light gray carbonate, which is crudely laminated parallel to the margin (Fig. 3C). The inner zone is 2 to 20 cm thick, composed of light brown dolomite. Small fenestrae occur within the inner zone. The thrombolite core consists of dark gray mesoclots (~1 cm in size) intermingled with abundant cm-scale patches of grainstone (Fig. 3D). The grainstone patches within the thrombolite are partly dolomitized. The interior core is circular to ellipsoidal-shaped (Fig. 3A, B). Either of the two rim zones may be absent in the longitudinal section (Fig. 3B). The boundaries between the rim and core are not sharp. Several dm-scale rimmed thrombolites accumulate both laterally and vertically, forming bioherms ca. 10 m in width. The thrombolites are separated from each other by thin oolitic grainstone (several cm to dm in width) via a sharp boundary.

4.1.1.2. Interpretation. The rimmed thrombolites most likely formed within the grainstone shoal as small patch reefs (e.g., Rees et al., 1989; Kruse et al., 1996; Adachi et al., 2011). The sharp boundaries between thrombolite and grainstone indicate that the thrombolites were eroded after lithification, through repetitive burial and exposure processes during their growth (cf., Bowlin et al., 2012). Grainstones in the core would have been imported onto the thrombolites during the growth, forming patches ~1 cm in size. This kind of grainstone–thrombolite relationship is different from the leiolite in which ooids are randomly distributed within the microbialite (Braga et al., 1995), but are rather similar to modern microbialites of Shark Bay within which sediments form mm- to cm-scale patches (Jahnert and Collins, 2011). The rim of the thrombolite would have developed after formation of the thrombolitic core, when the distance between the cores is sufficiently close (e.g., Camoin and Montaggioni, 1994; Riding and Tomás, 2006). Very high energy conditions induced by the narrow distance between the cores (less than a few dm) and phototropism by the calcified microbes

(Awramik and Vanyo, 1986; Woo and Chough, 2010), promoted formation of laminated rim (crust) on the core.

4.1.2. Grainstone-patch thrombolite

4.1.2.1. Description. The grainstone-patch thrombolite forms an irregular mound, imbedded within grainstone with which it has sharp boundaries (Fig. 4A). Mound size ranges from 10 to 100 cm. The thrombolites are distributed within the grainstone at distances of a few decimeters to meters. At the mesoscale, grainstone-patch thrombolite is similar to the core of rimmed thrombolite; dark gray microbial mesoclots occur within the thrombolite, together with grainstone patches 1 to 2 cm in size (Fig. 4B). The outer part of the thrombolite (~1 cm in width) does not contain grainstone patches.

4.1.2.2. Interpretation. The textural similarity between the core of rimmed thrombolite and the grainstone-patch thrombolite suggests that the grainstone-patch thrombolite formed in environments similar to those in which the rimmed thrombolite formed.

4.1.3. Dendritic thrombolite

4.1.3.1. Description. The dendritic thrombolite (or dendrolite) is characterized by irregular mounds (10–100 cm wide) with sharp and ragged boundaries, imbedded in limestone conglomerate (Fig. 5A, B). Dark gray dendritic mesoclots (3 to 6 mm) occur with light gray matrix in the dendritic thrombolite (Fig. 5C). Dendritic mesoclots are laterally connected, forming stacked layers 3–5 mm thick. Matrix is composed of botryoidal structures separated from each other by dark gray matrix.

4.1.3.2. Interpretation. The dendritic thrombolites most likely formed by microbial calcification (Riding, 1991b; Riding, 2000). Dendritic mesoclots may have formed by an upward-expanding growth tendency of the calcified microbes (Howell et al., 2011). The occurrence of limestone conglomerates surrounding the dendritic thrombolites, together with erosional sharp boundaries, indicate that the dendritic thrombolite

Table 1
Summary of the three types of thrombolites in the Zhushadong Formation.

Thrombolite types	Macroscale description	Mesoscale description	Microscale description	Interpretation
Rimmed thrombolite	Characterized by rim consisting two zones and thrombolitic core (Fig. 3A–C); core is circular or ellipsoidal in transverse section and bowl-like in longitudinal section (ca. 60 cm in width); outer zone of rim (1–5 cm in width) and inner zone (2–20 cm in width) are often absent in longitudinal section; thin oolitic grainstone (few cm to dm in width) occurs between bioherms; boundaries between the rim, core, and grainstone are usually sharp; several dm-scale thrombolites accumulate and form large bioherm (ca. 10 m in width)	Outer zone of rim composed of light gray carbonate with crude lamination; inner zone of rim comprises light brown dolomite with small fenestrae and very crude lamination; core contains dark gray mesoclot (~1 cm) and cm-scale patch-shaped grainstone (Fig. 3C, D)	Core: *Epiphyton* and *Kordephyton* form colony of ~500 μm in size, surrounded by tubiform microbes (Fig. 6); ooids within grainstone patches 80–200 μm in size. Rim: *Amgaina* directs normal to the laminations (Fig. 8B); boundary between the outer and inner zones gradual (Fig. 8A)	Small patch reefs within grainstone shoal (e.g., Kruse et al., 1996; Rees et al., 1989; Adachi et al., 2011); thrombolites experienced repetitive burial and exposure processes (cf. Bowlin et al., 2012); rims formed after formation of core under high energy conditions
Grainstone-patch thrombolite	Irregularly shaped mound (10 to 100 cm in width and height) (Fig. 4A); surrounded by grainstone via sharp boundary; each mound apart from each other with few dm to m in distance in between	Dark gray mesoclot (~1 cm) and cm-scale patch-shaped grainstone (Fig. 4B); grainstone patches absent in the outer part (~1 cm in width); similar to core of rimmed thrombolite	Similar to core of rimmed thrombolite (Fig. 6)	Patch reef within grainstone shoal; similar environment to that of rimmed thrombolite
Dendritic thrombolite	Irregularly shaped mound (10 to 100 cm in width and height) (Fig. 5A, B); surrounded by limestone conglomerates via sharp boundaries	Dark gray mesoclot (3–6 mm) of upward widening dendritic shape (Fig. 5C); surrounded by light gray matrix	Mixed *Epiphyton* and *Tarthinia* colonies (Fig. 7); tubiform microbes occur between the other microbial colonies	Formed by microbial calcification (Riding, 1991b, 2000)

developed under high-energy conditions together with deposition of the limestone conglomerates. The absence of grainstone patches within the dendritic thrombolite is most likely due to differences in formative processes; trapping and binding processes within the dendritic thrombolite would not have been strong enough to trap large limestone intraclasts.

4.2. Microscale characteristics

Several calcified microbes are identified in the Zhushadong thrombolites, including *Epiphyton*, *Kordephyton*, tubiform microbe, *Tarthinia*, *Bija*, *Renalcis* and *Amgaina* (Table 1). *Epiphyton*, *Kordephyton*, and the tubiform microbe are dominant, whereas the remainders are minor. Occurrences of calcified microbes differ according to the macro- and mesostructure. Three groups of calcified microbes are recognized: 1) core of rimmed thrombolite and grainstone-patch thrombolite, 2) dendritic thrombolite, and 3) rim of rimmed thrombolite. The core of rimmed thrombolite and grainstone-patch thrombolite generally consist of *Epiphyton*, *Kordephyton*, and the tubiform microbe, with minor *Bija* and *Renalcis*. Dendritic thrombolite is mainly constructed by *Epiphyton*, *Tarthinia*, and the tubiform microbe. The rim of rimmed thrombolite is composed of *Amgaina*.

4.2.1. Calcified microbes

4.2.1.1. Epiphyton.

4.2.1.1.1. Description. *Epiphyton* is a branching, dendritic filamentous structure composed of dense micrite (Figs. 6A, B, G and 7A, C, D). Each branch is ~200 μm in length and 25–35 μm in width. Several *Epiphyton* occur together, forming relatively large colonies ~500 μm in size (Fig. 6A). When *Epiphyton* is dominant within the thrombolite, several colonies are connected to form mm-scale colonies (Fig. 7C). Generally *Epiphyton* branches upward. In some cases, *Epiphyton* colonies form chambered structures, similar to those of *Renalcis* (Fig. 6G) (cf., Woo et al., 2008; Adachi et al., 2014). *Epiphyton* is by far the dominant calcified microbe within Zhushadong thrombolites. It occurs in every type of thrombolite, except in the rim of rimmed thrombolite.

4.2.1.1.2. Discussion. *Epiphyton* occurs extensively during the Cambrian, Early Ordovician, and Late Devonian (Riding, 1991a). Based on their size, morphology, and modern analogs, *Epiphyton* is regarded as a cyanobacterium (Riding, 1991a; Laval et al., 2000). Interestingly, Zhushadong *Epiphyton* is noticeably smaller than its descendants in the Cambrian Series 3 Zhangxia Formation, which have branches 40–80 μm in width (see Section 5.2.2) (Woo et al., 2008).

4.2.1.2. Kordephyton

4.2.1.2.1. Description. *Kordephyton* is characterized by a group of numerous thin micritic filaments which are generally aligned in a subvertical to vertical direction (Fig. 6A, C, D). The approximate thickness of each filament is 5–15 μm, and the length of each branch is 300–800 μm. They usually form relatively circular colonies (~500 μm in width). Many of the filaments appear fuzzy in thin sections with outlines that are difficult to identify. Sparite occurs between the separated filaments. Most of the micritic filaments appear solid, although a few are tubular (Fig. 6C). *Kordephyton* is often associated with *Epiphyton* colonies and/or grainstone patches, and commonly occurs in the core of rimmed thrombolite and grainstone-patch thrombolite.

4.2.1.2.2. Discussion. *Kordephyton* has been recognized in the Terreneuvian and Cambrian Series 2 deposits (Riding and Voronova, 1984; Mankiewicz, 1992; Elicki, 1999). It has been grouped with *Epiphyton* and *Angulocellularia* (Riding and Voronova, 1985) or *Botomaella* (Elicki, 1999; Riding, 2001), for its dendritic structures. Due to its fuzzy outline, however, it can be difficult to identify whether or not its filaments branch. On the other hand, *Kordephyton* has been described as a kind
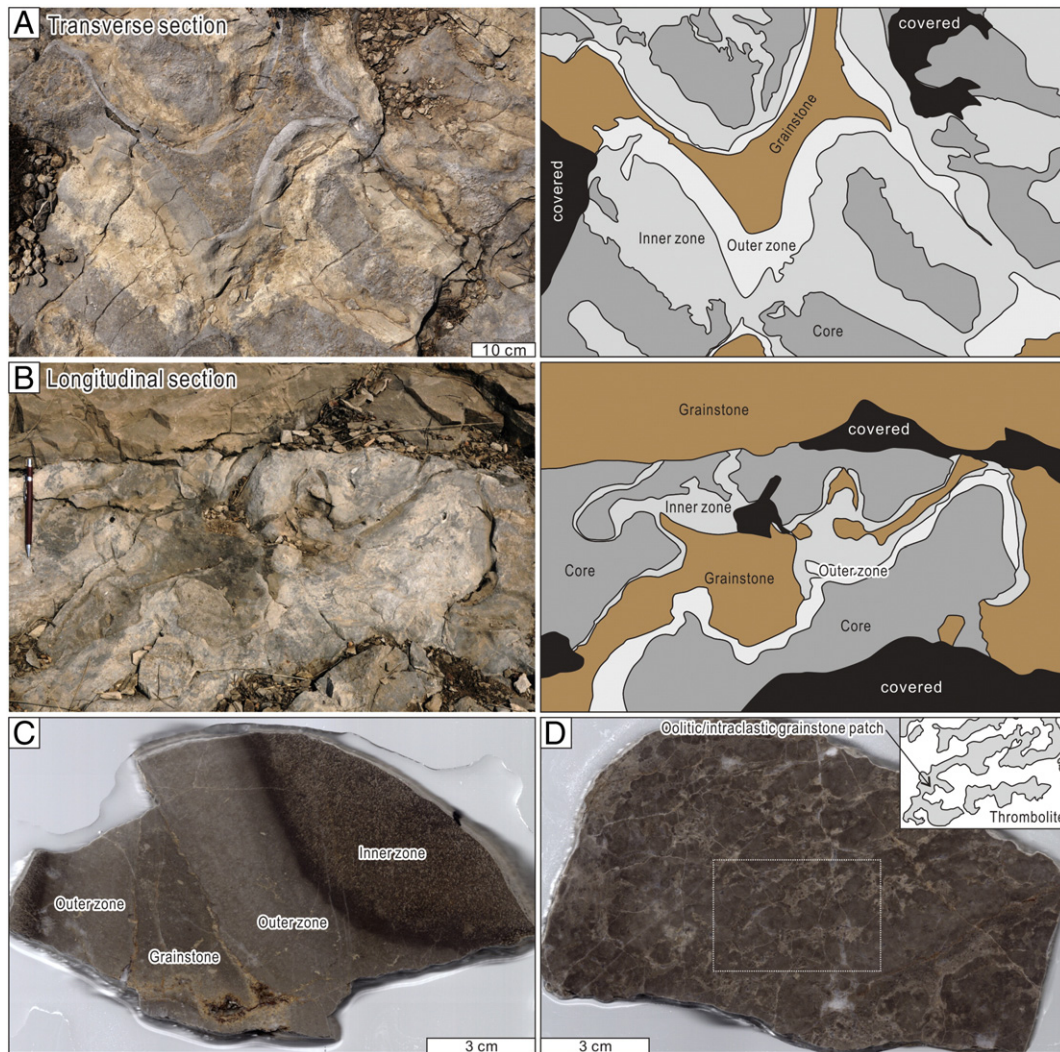
Fig. 3. Rimmed thrombolite. (A) Photograph of transverse section and sketch. (B) Photograph of longitudinal section and sketch. Pencil is 14.5 cm in length. (C) Slab of rim and grainstone, showing sharp intervening boundaries. (D) Slab of the thrombolitic core, showing dark gray mesoclots and light brown, partly dolomitized grainstone patches.

of *Girvanella* due to its thin micritic filaments (Read and Pfeil, 1983; McMenamin et al., 2000). The occurrence of tubular filaments in the Zhushadong *Kordephyton* may suggests that *Kordephyton* can be grouped with *Girvanella*, in which case the calcified sheaths of filamentous cyanobacteria could be modern analogs (Riding, 1977).

4.2.1.3. Tubiform microbe

4.2.1.3.1. Description. Tubiform microbes display circle to boudin-like shapes, composed of thin micritic walls (10–20 μm thick) and surrounding sparite (Figs. 6D, E, F and 7A). The tube length is 100–1000 μm and width is 50–100 μm. Although the micritic walls usually form closed curves and boudin-like shapes, the walls are sometimes disconnected and open curves (Fig. 6E). The boudin-like shapes locally branch and form X- or Y-shaped structures (Fig. 6E). They usually occur as a small group of around 10 to 20 closely spaced individuals. Interestingly, they are generally not mutually attached, and are separated by micrite or microsparite. In some cases, they form large groups of more than several hundred individuals, which are loosely connected or dispersed within micrite. The tubiform microbes usually surround other microbial colonies or grainstone patches. They occur in the core of rimmed thrombolite, grainstone-patch thrombolite, and dendritic thrombolite.

4.2.1.3.2. Discussion. The tubiform microbe shares some features with *Bevocastria*, described by Garwood (1931) from the Early Carboniferous;

it is similar to *Bevocastria* in diameter and in its irregularly sinuous arrangement that forms closely packed, tangled masses. However, the distinguishing feature of *Bevocastria* is regular constrictions of the tube. These may be present in the tubiform microbe, but are not obviously present. In their absence, it is difficult to definitely confirm the tubiform microfossil as *Bevocastria* (see also Feng et al., 2010, p. 575).

4.2.1.4. Bija

4.2.1.4.1. Description. Bija is characterized by thick, branching tubes filled by sparite (Fig. 6F). The tube width is about 50–70 μm, and the length is ca. 1 mm. The walls are thin and micritic, ca. 8–15 μm in width. *Bija* displays relatively irregular circles in cross-section. Usually 10 to 30 branches occur together, forming a large-fan shaped colony ca. 2–4 mm in width. *Bija* usually occurs near the grainstone patches, in the core of rimmed thrombolite and grainstone-patch thrombolite.

4.2.1.4.2. Discussion. Calcified microbes somewhat similar to *Bija* are known from various Phanerozoic periods, and with different names; *Bija* in the Cambrian, *Hedstroemia* in the Cambrian and Silurian, *Ortonella* in the Carboniferous, and *Cayeuxia* in the Triassic to Cretaceous (Riding, 1991a; Flügel, 2004). All of these are characterized by relatively thick branching tubes. They have been compared with modern rivulariacean cyanobacteria (Riding, 1991a; Riding and Fan, 2001). These calcified microbes with different names may indicate similar
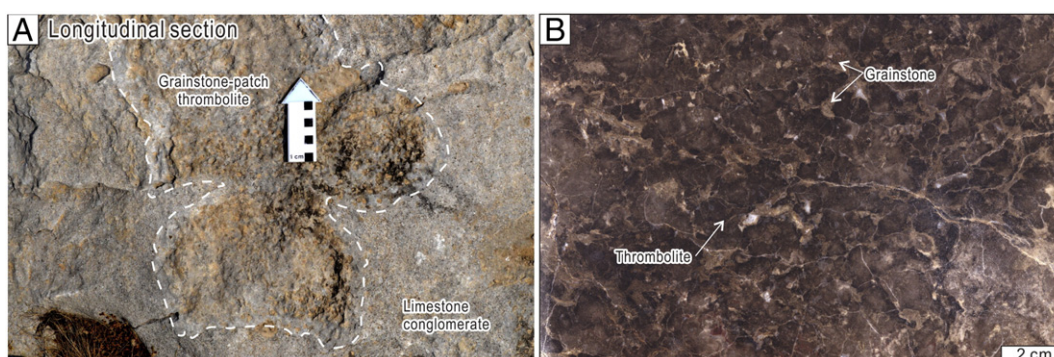
Fig. 4. Grainstone-patch thrombolite. (A) Photograph of longitudinal section. (B) Slab of the thrombolite, showing similar texture to that of the core of rimmed thrombolite.

structures, but detailed comparisons have not yet been made. In this study, we use the name *Bija* to indicate these calcified microbes, based on their relatively irregular cross-sections (Mankiewicz, 1992).

4.2.1.5. Tarthinia

4.2.1.5.1. Description. Tarthinia is characterized by its botryoidal, chambered structure with thick fibrous microsparitic walls, with a center of coarser sparite. The microsparite crystals are generally oriented normal to the wall. Each chamber is about 250–350 μm in diameter, and the wall thickness is about 50–100 μm. Chambers are separated from one another by thin areas of micrite and/or sparite. Typically, several colonies of *Tarthinia* occur together, forming a large colony ~3 mm in size. *Tarthinia* occurs within the dendritic thrombolite.

4.2.1.5.2. Discussion. Tarthinia is similar to *Renalcis* in size and morphology, but differs in its thicker and apparently microsparitic wall (Riding, 1991a; Mankiewicz, 1992). On the other hand, it has been suggested that *Tarthinia* might be diagenetic alternation products of calcified microbe colonies that originally consisted of micrite (Ezaki et al., 2003).

4.2.1.6. Renalcis

4.2.1.6.1. Description. Renalcis has a characteristic botryoidal structure, consisting of micritic walled chambers filled with microsparite. Each chamber is 150–350 μm in diameter, and the wall thickness is 30–40 μm. Several tens of colonies often occur together, occupying

areas a few mm in width. *Renalcis* rarely occurs in the grainstone-patch thrombolite.

4.2.1.6.2. Discussion. Renalcis has been regarded as a cyanobacterium by many authors, based on its size and morphology, but the absence of a definite modern analog makes it difficult to confidently place it in cyanobacteria (Riding, 1991a). Recently chambered *Epiphyton*, showing somewhat similar morphology to that of *Renalcis*, has been reported, suggesting the possibility that *Renalcis* might be a diagenetically altered form of chambered *Epiphyton* (Pratt, 1984; Woo et al., 2008; Adachi et al., 2014). On the other hand, it has also been suggested that *Renalcis* and *Epiphyton* may represent different stages in the life cycle of cyanobacteria (Luchinina, 2009).

4.2.1.7. Amgaina

4.2.1.7.1. Description. Amgaina is characterized by chambered, botryoid structures with a micritic wall (Fig. 8). The width of each chamber is ca. 80–100 μm, and the wall is 15–20 μm thick. The chambers are attached, and form branching structures, ca. 600 μm in length. Microsparite fills the chambers. *Amgaina* is only found in the rim of rimmed thrombolite.

4.2.1.7.2. Discussion. Several calcified microbes consist of irregularly branching, chambered structures, including *Chabakovia*, *Parachabakovia*, *Taninia*, and *Amgaina* (Korde, 1973; Pratt, 1984). Some of these microbes also resemble branching *Renalcis* (Riding, 1991a). *Amgaina* in this study is identified based on its relatively large size (ca. 80–100 μm in width), which is larger than the other similar genera (e.g., the ca. 40 μm width of *Parachabakovia*) (A.Y. Zhuravlev, pers. comm.).
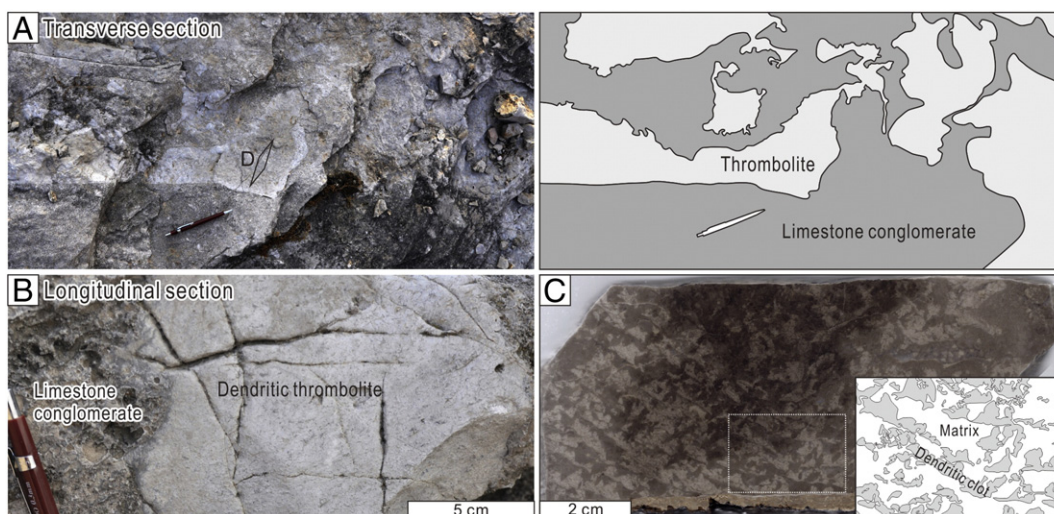
Fig. 5. Dendritic thrombolite. (A) Photograph of transverse section and sketch. Pencil is 14.5 cm in length. (B) Photograph of longitudinal section. (C) Slab showing dark gray dendritic mesoclots and light gray matrix.
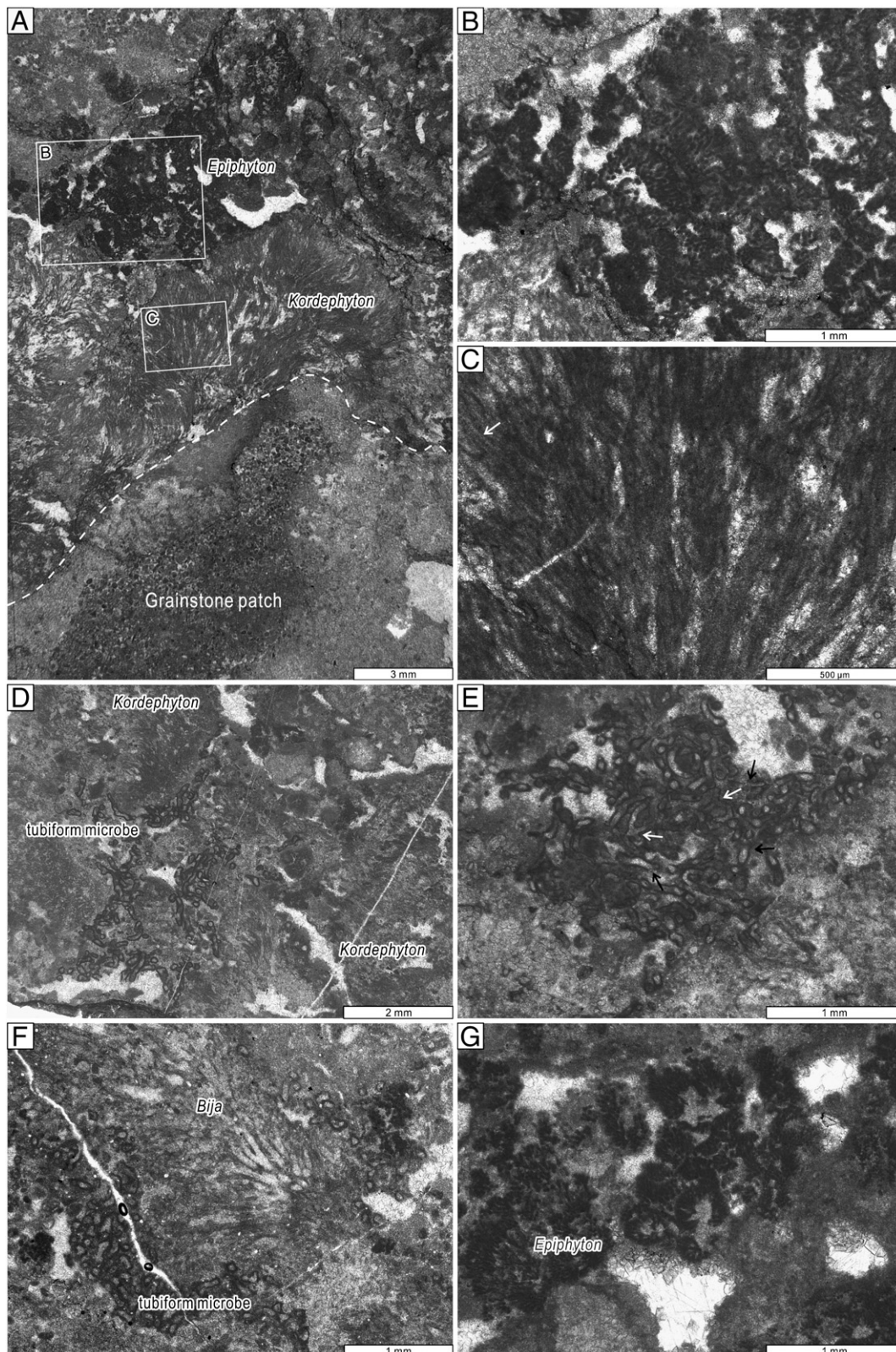
Fig. 6. Microphotograph of calcified microbes in the core of rimmed thrombolite and grainstone-patch thrombolite. (A) Microbial colonies occurring on top of a grainstone patch. *Kordephyton* directly attached to the top of the grainstone, which in turn is overlain by *Epiphyton*. The outer part of the grainstone patch is dolomitized. (B) A close-up of *Epiphyton*, showing branching dendritic structures. (C) Close-up of *Kordephyton*. The micritic filaments composing *Kordephyton* are mostly fuzzy, although some retain tubular structure (arrow). (D) *Kordephyton* colonies surrounded by tubiform microbes. (E) Close-up of tubiform microbe, which is composed of thin micritic walls and filled with microsparite. Note branching structures (white arrow) and disconnected walls (black arrow) (F) *Bija*, surrounded by tubiform microbe colonies. (G) Characteristically chambered *Epiphyton*.
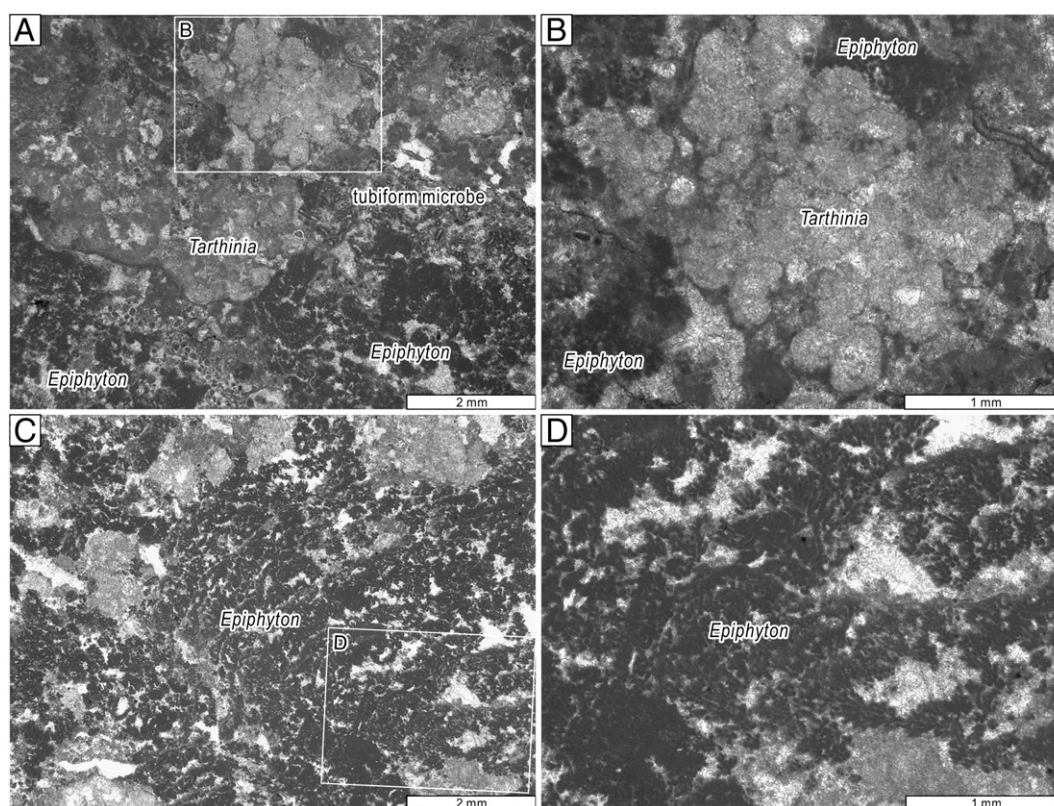
Fig. 7. Photomicrograph of dendritic thrombolite. (A) *Epiphyton* and *Tarthinia*, with tubiform microbes occurring in the interspace between them, together with some ooids. (B) Close-up of *Tarthinia*, surrounded by *Epiphyton* and micrite. (C) *Epiphyton* colonies forming dendritic mesoclots. (D) Close-up photomicrograph showing fan-shaped *Epiphyton*.

4.2.1.8. Razumovskia

4.2.1.8.1. Description. Razumovskia is characterized by several thin, laterally or vertically curled filaments. Its length is 500–1000 μm and width 5–20 μm. In our specimens, the filaments are rarely tubiform. The orientation of filaments vary, but is generally subvertical. Filament thickness is irregular. They are embedded in sparite or micrite. *Razumovskia* occurs rarely within the core of rimmed thrombolite and grainstone-patch thrombolite, forming thin arcuate rafts scattered in the cement (cf., Gandin et al., 2007).

4.2.1.8.2. Discussion. Razumovskia is characterized by bundles of filaments with a curved, "felted" fabric (Korde, 1973; Mankiewicz, 1992). Tubiform filaments of *Razumovskia* are similar to those of *Girvanella*, which suggests their close affinity (Mankiewicz, 1992).

4.2.2. Occurrences of calcified microbes within thrombolite

4.2.2.1. Core of rimmed thrombolite and grainstone-patch thrombolite

4.2.2.1.1. Description. Within these thrombolite fabrics, calcified microbes are usually associated with oolitic grainstone patches ca. 2 mm in size (Fig. 6A). The ooids composing these patches are 80–200 μm in size and are not eroded. *Epiphyton* and *Kordephyton* colonies often show upward growth. The tubiform microbes mainly occur along the boundaries of microbial colonies and grainstone patches, forming thin bands 1–5 mm in width (Fig. 6D, F). A few *Bija* colonies are found near the grainstone patches or margins of the thrombolite. *Renalcis* and *Razumovskia* rarely occur within the thrombolite. The outer parts of the grainstone patches (1–3 mm in width) are usually dolomitized.

4.2.2.1.2. Interpretation. Epiphyton and *Kordephyton* grew on top of grainstone patches or other microbial colonies, forming thrombolitic mesoclots (Kennard and James, 1986; Elicki, 1999; Álvaro et al., 2006). *Epiphyton* overgrowth on other microbial colonies is common in the early Cambrian, reflecting their role as frame-builder (Kobluk, 1985;

Elicki, 1999). Tubiform microbes encrusted the other microbial colonies or rarely the grainstone patches. *Bija* formed under relatively high energy conditions are affected by grainstone input. The uneroded ooids within the grainstone patches indicate that the ooids formed in nearby grainstone shoals and were transported into the thrombolites during thrombolite formation. The outer parts of the grainstone patches were subsequently selectively dolomitized.

4.2.2.2. Dendritic thrombolite

4.2.2.2.1. Description. The dendritic thrombolite is characterized by a mixture of *Epiphyton* and *Tarthinia* colonies (Fig. 7A, B). *Epiphyton* usually occurs as dark gray dendritic mesoclots in slabs, whereas *Tarthinia* form as a light gray matrix with a botryoidal structure. *Epiphyton* branches upward to form fan-shaped structures. Dendritic mesoclots consist of stacked *Epiphyton* colonies (Fig. 7C, D). *Tarthinia* is surrounded by *Epiphyton* or micrite. Tubiform microbes mainly occur between the *Epiphyton* and *Tarthinia* (Fig. 7A). The tubiform microbes are in some cases mixed with *Epiphyton* colonies (Fig. 7A).

4.2.2.2.2. Interpretation. The undisturbed upward widening pattern of *Epiphyton* suggests that it grew prior to *Tarthinia*, forming frameworks (Elicki, 1999). *Tarthinia* then filled interspaces between the *Epiphyton* frameworks. Tubiform microbes encrusted other microbial colonies (e.g., *Epiphyton* or *Tarthinia*) while the underlying microbial colonies were still active, as shown by mixed occurrence of *Epiphyton* and tubiform microbes. This type of calcified microbe assemblage is similar to that of *Tarthinia–Epiphyton–Gordonophyton–Renalcis* boundstone from Mongolia (Cambrian Series 2, Stage 3) (Wood et al., 1993), except that the latter lacks tubiform microbes.

4.2.2.3. Rim (crust) of rimmed thrombolite

4.2.2.3.1. Description. The rims of the rimmed thrombolites are characterized by *Amgaina*, oriented normal to the laminations. Many of the
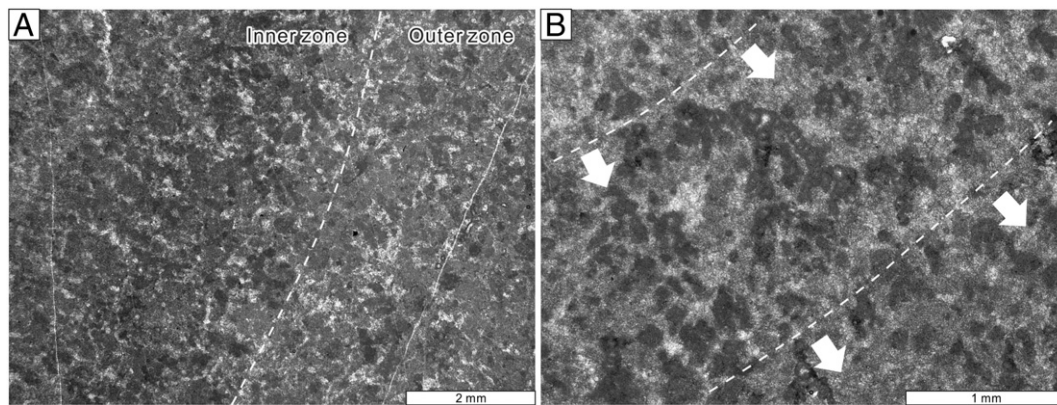
Fig. 8. Photomicrograph of the rim of rimmed thrombolite. (A) Boundary between the inner and outer rim zones, marked by a dotted line. (B) *Amgaina* in the inner zone. Dotted lines indicate lamination. *Amgaina* is oriented normal to the lamination, indicating outward growth.

Amgaina are poorly preserved, showing only micritic clotted structures. The boundary between the outer and inner rim zones is gradual at the microscale, whereas the boundary between the rim and grainstone is sharp.

4.2.2.3.2. Interpretation. Rims (or crusts) may have formed between the thrombolitic cores, where energy conditions were high (cf., Camoin and Montaggioni, 1994). Other calcified microbes within the cores could not endure these conditions and *Amgaina* occurred in their place (cf., Woo and Chough, 2010). The branching direction of *Amgaina* indicates that they grew outward, away from the core. The gradual boundary between the outer and inner rim zones suggests that diagenetic effects, such as dolomitization of the inner zone, may have caused the differences between the outer and inner zones.

5. Discussion

5.1. Reefs in the Cambrian of the North China Platform

Various microbial reefs occur within the Zhushadong Formation and the overlying Cambrian successions (Fig. 1B). Microbial laminites and stromatolites formed during the Cambrian Series 2 and the early Cambrian Series 3 (Zhushadong and Mantou formations), but no calcified microbes have been reported from them (Lee and Chough, 2011; Chang et al., 2012). During the middle–late Cambrian Series 3 (Zhangxia Formation), various microbial reefs flourished, including *Epiphyton* framestone, thrombolite, dendrolite, and stromatolite; some of which contain reef-building metazoans such as siliceous sponges and stem-group cnidarian (*Cambroctoconus*) (Fig. 9) (Mu et al., 2003; Woo et al., 2008; Woo, 2009; Park et al., 2011; Hong et al., 2012). These microbial reefs occupy a significant volume (up to 1/3) of the ca. 180 m thick microbial reef–oolite succession of the Zhangxia Formation (Woo et al., 2008). *Epiphyton* occurs dominantly within the Zhangxia microbial reefs, together with rare *Renalcis* and *Girvanella* (Woo et al., 2008; Woo and Chough, 2010; Howell et al., 2011). The Zhangxia carbonate platform was drowned during the late Cambrian Series 3 (Gushan Formation) (Chen et al., 2011, 2012), but resurged in a series of maze-like maceriate reefs, with siliceous sponges and various microbial components including *Girvanella* and rare *Tarthinia*, during the Furongian (Chaomidian Formation) (Lee et al., 2010, 2012, in press; Chen et al., 2011).

Until now, calcified microbes in the Cambrian succession of the North China Platform have only been reported from the Zhangxia and Chaomidian formations (e.g., Woo et al., 2008; Lee et al., 2010, in press). Recently, Liu and Zhang (2012) reported *Girvanella* from ooids and oncoids of the middle Mantou Formation of Shaanxi Province (Maochuangian Stage; Cambrian Series 3, Stage 5), but even this occurrence postdates the calcified microbes of the present study. Therefore, these Zhushadong thrombolites in the Sunmayu section record the earliest calcified microbes of their kind (Cambrian Series 2, Stage 3) reported from the North China Platform.

On the other hand, no archaeocyath has ever been reported from the North China Platform, although calcified microbes formed reefs in the platform during the Cambrian Series 2. The reasons for this absence of archaeocyaths from the platform are remain enigmatic. Paleomagnetic data for the Sino-Korean Block suggest that the platform was located at a low latitude (<30°) during the Cambrian, which would appear to rule out low temperature as a cause (Zhao et al., 1992; Huang et al., 2000; Yang et al., 2002). The harsh depositional environments of the Zhushadong Formation (e.g., abundant siliciclastic input and tidal effect) also do not explain the absence of archaeocyaths, since they appear to have been able to tolerate even siliciclastic environments (Lasemi and Amin-Rasouli, 2007) and tide-dominated conditions (Rowland, 1984). Since archaeocyaths occurred in most major continental blocks during the Terreneuvian and Cambrian Series 2 (Gandin and Debrenne, 2010), and some are often considered cosmopolitan (Debrenne and Rozanov, 1983; Zhuravlev, 1986; Rowland and Gangloff, 1988), the dispersal ability of archaeocyaths should have been sufficient to reach the North China Platform. Further investigations into the Cambrian Series 2 deposits of the North China Platform, and studies of archaeocyaths elsewhere, may eventually resolve the puzzling absence of archaeocyaths from the North China Platform. Nonetheless, this provides a unique chance to examine the Cambrian diversification of calcified microbes in the absence of archaeocyaths (Section 5.2.2).

5.2. Controls on diversification of calcified microbes

Microbial reefs of the Zhushadong Formation are similar to those of the Zhangxia Formation (Cambrian Series 3, Drumian–Guzhangian stages), since both of them are characterized by thrombolitic texture and the calcified microbe *Epiphyton* (Figs. 1B and 9). However, these microbial reefs are different in terms of occurrence and composition. Thrombolites rarely occur in the Zhushadong Formation (only within a 3 m thick interval that extends laterally over ca. 1 km²), whereas microbial reefs are abundant within the Zhangxia Formation (a 180 m thick interval, correlated over 100 km²). The diversity of calcified microbes within the reefs is, however, opposite. At least eight types of calcified microbes occur within the Zhushadong thrombolites, whereas only three types are recognized in the Zhangxia microbial reefs, with *Epiphyton* predominating (Table 2).

It is interesting to note that *Epiphyton* displays different characteristics in the Zhushadong and Zhangxia formations. *Epiphyton* in the Zhangxia Formation is more diverse (4 different types) and about twice as large as those in the Zhushadong Formation (40–80 μm vs. 25–35 μm filament diameter) (Woo et al., 2008). These 4 types of *Epiphyton* may include different genera (e.g., *Gordonophyton*) (Woo
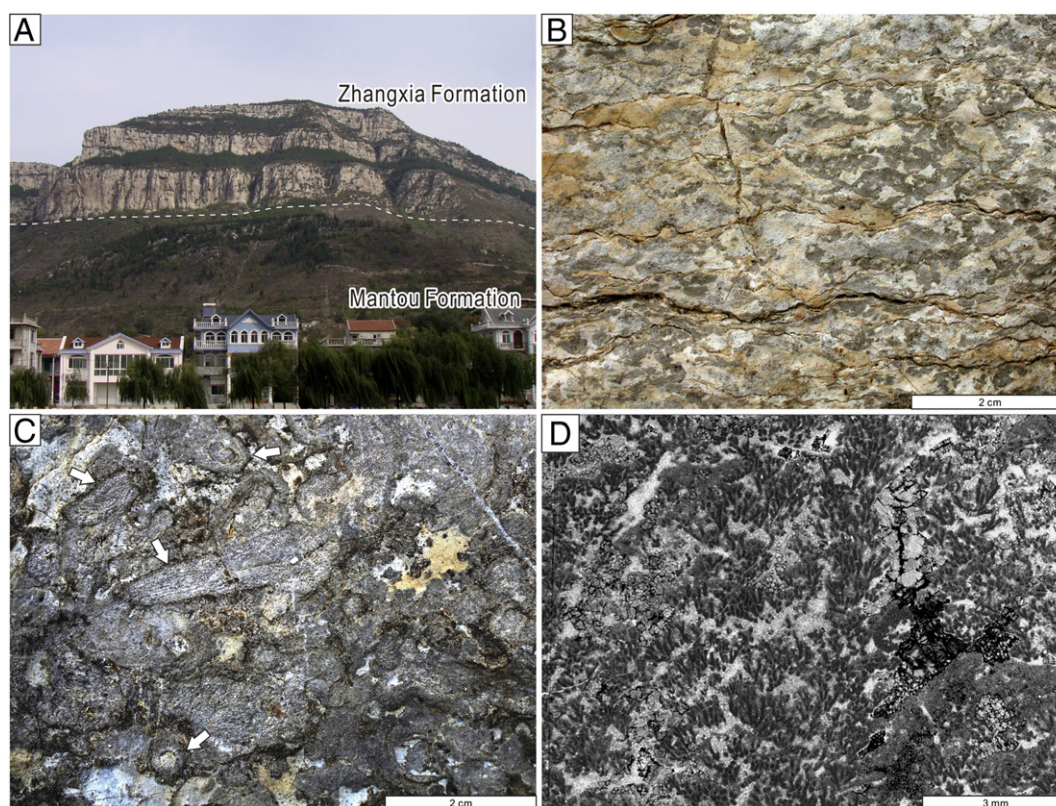
Fig. 9. Microbial reefs of the Zhangxia Formation (Cambrian Series 3) in the Jinan region, Shandong Province, China. (A) In megascale, the Zhangxia Formation is represented by a thick microbial reef-oolite succession. (B) Typical thrombolite in the Zhangxia Formation. (C) Siliceous sponges (white arrow) within *Epiphyton* framestone. (D) *Epiphyton*, showing branched structure.

et al., 2008). The overall diversity of calcified microbes in the Zhangxia Formation is, however, lower than those in the Zhushadong Formation. Although the Zhangxia *Epiphyton* may represent four different genera, they can all be classified within the *Epiphyton* group (Riding, 1991a). On the other hand, the characteristic calcified microbes in the Zhushadong Formation represent four different groups (*Epiphyton*, *Girvanella*, *Hedstroemia*, and *Renalcis* groups) (Riding, 1991a), of which each groups is locally significant within the reefs.

Why then, was the diversity of calcified microbes lower in the Zhangxia Formation even though they flourished? The diversity and abundance of these calcified microbes could have been controlled by two main factors: local depositional environments and evolutionary change in calcified microbes determined by global environmental conditions.

5.2.1. Depositional environments

The Zhushadong Formation formed during the initial stage of transgression, with the input of siliciclastic sediments in supratidal to subtidal settings (Lee and Chough, 2011). Microbial reefs would not have flourished in these dynamic (tidal effects) and stressful (siliciclastic input) conditions, and this limited the development of thrombolites in the Zhushadong Formation (cf., Elicki, 1999). On the other hand, the relatively harsh environments of the Zhushadong Formation could have promoted diversification of the calcified microbes, since diversity is usually higher under intermediate levels of disturbance (e.g., siliciclastic input, tidal effect, and grazers) than under either high or low levels of disturbance (intermediate disturbance hypothesis) (Connell, 1978; Rogers, 1993; England et al., 2008).

In this view, the thrombolites in the Zhushadong Formation would have diminished due to excessive siliciclastic input during the late Cambrian Series 2–early Cambrian Series 3 (Mantou Formation) (Fig. 1) (Lee and Chough, 2011). Due to this event, the diversity of the Zhushadong calcified microbes would also have decreased. The

microbialites recovered when siliciclastic input ceased and a stable carbonate platform (Zhangxia Formation) formed during the middle Cambrian Series 3 (Woo, 2009; Chough et al., 2010). The surviving microbe taxa (e.g., *Epiphyton*) flourished and formed reefs within the Zhangxia Formation under favorable conditions for microbial growth (low levels of disturbance). However, the diversity of calcified microbes decreased due to the low levels of disturbance.

5.2.2. Global environmental conditions

Together with the extinction of archaeocyaths at the end-Cambrian Series 2, the diversity of calcified microbes decreased from ca. 20 (Stage 4) to ca. 13 genera (Stage 5) (Zhuravlev, 1996; Riding, 2001) (Fig. 10). The decrease in calcified microbe diversity during the Cambrian Series 2 and 3 in the North China Platform can be correlated with global trends; calcified microbes that occur only during the Terreneuvian and Cambrian Series 2 also occur in the Cambrian Series 2 Zhushadong Formation (e.g., *Kordephyton*, *Bija*, *Amgaina*, and *Razumovskia*) (Mankiewicz, 1992; Zhuravlev, 1996; Riding, 2001), whereas none of them has been reported from the Cambrian Series 3 Zhangxia Formation (Woo et al., 2008).

It has been suggested that calcified microbe diversity decreased when archaeocyaths became extinct, due to the loss of the ecological niche created by archaeocyaths and to the reduction of stress levels to calcified microbes caused by the extinction of tiny grazers (Zhuravlev, 1996). In the case of the North China Platform, where archaeocyaths are absent, it seems most likely that calcified microbe diversity was not affected by the extinction of archaeocyaths themselves. Also, the presence of reef-building metazoans (siliceous sponges and *Cambroctoconus*) within the Zhangxia microbial reefs suggests that loss of the ecological niche created by archaeocyaths was not critical to some of the calcified microbes that disappeared during the extinction event, since these other reef-building metazoans could have provided a similar ecological niche to that of archaeocyaths. The extinction of tiny grazers may have

Table 2
Comparison of microbial reefs in the Zhushadong Formation (Cambrian Series 2) and the Zhangxia Formation (Cambrian Series 3) in Shandong Province, China.

	Zhushadong Formation (This study)	Zhangxia Formation (Woo et al., 2008, 2010; Howell et al., 2011; Park et al., 2011)
Age	Cambrian Series 2 (Stage 3)	Cambrian Series 3 (Drumian–Guzhangian)
Abundance of microbialites	One horizon only (3 m thick), with limited occurrence (up to 1 km²)	Ca. 30% of entire Formation (180 m thick)
Macrostructure	Small domal/irregular mound, rimmed	Thin-flat layer, domal, upward-widening fan, single or stacked bioherm
Mesostructure	Grainstone-patch, clotted, dendritic, laminated rim	Clotted, dendritic, laminated
Calcified microbes	*Epiphyton*, *Kordephyton*, tubiform microbe, *Bija*, *Tarthinia*, *Renalcis*, *Amgaina*, and *Razumovskia*	*Epiphyton*, *Renalcis*, and *Girvanella*
Co-occurring reef-building fauna	None	Siliceous sponge, stem-group cnidarian (*Cambroctoconus*)

homogenized microbial communities, and some calcified microbes previously suppressed by grazers could then have flourished and dominated other calcified microbes, resulting in a decrease in calcified microbe diversity (Zhuravlev, 1996). However, this suggestion requires further investigation.

On the other hand, global events that caused mass extinction could have directly decreased the diversity of calcified microbes (Zhuravlev and Wood, 1996; Zhuravlev, 2001). These events include anoxic conditions caused by global transgression (Sinsk event) (Zhuravlev and Wood, 1996), followed by a reduction in shallow environments due to regression (Hawke Bay event) (Zhuravlev and Wood, 1996; Álvaro et al., 2000; Álvaro and Debrenne, 2010). In addition, a major volcanic eruption (Kalkarindji continental flood basalt province, northern Australia) has been suggested as a cause of the extinction event (Glass and Phillips, 2006; Hough et al., 2006; Kruse and Zhuravlev, 2008; Adachi et al., 2014). Significant amounts of nutrients (e.g., Fe, Mn, Si, P, NH_4) and greenhouse gasses (e.g., H_2O, CO_2) from volcanic eruptions may have stimulated phytoplankton blooms that induced anoxic and greenhouse conditions (Kruse and Zhuravlev, 2008). Anoxic conditions could have selectively induced extinction of cyanobacteria that are less tolerable to anoxic conditions (Thomas et al., 2005).

The survived microbial communities would have diversified again and occupied the empty ecological niche created by the extinction of competing microbial taxa (adaptive radiation) (Schluter, 2000). The four different types of Zhangxia *Epiphyton*, that are distributed unevenly within the bioherm, suggest that they were adapted to differing ecological niches (Woo and Chough, 2010). The larger size of Zhangxia *Epiphyton* compared with their ancestors in the Zhushadong Formation was probably due to a removal of constraints (e.g., predation or competition) on their size (insular gigantism) (Bowen and Van Vuren, 1997), as a result of the extinction event. These possibilities warrant a further examination of other calcified microbes in the Cambrian Series 2 and 3 elsewhere to determine their morphologic variations in terms of ecological change.

6. Conclusions

The Cambrian Series 2 Zhushadong thrombolites yield the earliest calcified microbe so far reported from the North China Platform. Diverse calcified microbes, including *Epiphyton*, *Kordephyton*, tubiform microbe, *Bija*, *Tarthinia*, *Renalcis*, *Amgaina*, and *Razumovskia*, occur in the thrombolites. The thrombolites formed within a grainstone shoal associated with repetitive burial and exposure processes on the sea floor. Whereas these eight calcified microbes occur in the Zhushadong Formation, only *Epiphyton*, *Renalcis*, and *Girvanella* are present in the overlying Zhangxia Formation (middle–late Cambrian Series 3). Nonetheless, although Zhangxia calcified microbes have lower diversity, they are very abundant. These temporal changes in calcified microbes most likely reflect changes in depositional environments and/or global environmental conditions. Stressful conditions in the Zhushadong Formation would have promoted diversification of calcified microbes, although it would also have suppressed their abundance and prevented them from forming large reefs. In contrast, the changes in global environments reflected by the end-Cambrian Series 2 extinction could have directly reduced the diversity of calcified microbes. But these surviving microbes were well adapted to the post-extinction environment, and as a result they were able to form thick and extensive reefs during the Cambrian Series 3 in the North China Platform.

Fig. 10. Global diversity of calcified microbes during the Cambrian. Modified after Zhuravlev (1996) and Riding (2001).

Appendix A. Supplementary data

Supplementary data associated with this article can be found in the online version, at http://dx.doi.org/10.1016/j.palaeo.2014.03.020. These data include Google maps of the most important areas described in this article.

References

Adachi, N., Ezaki, Y., Liu, J., 2011. Early Ordovician shift in reef construction from microbial to metazoan reefs. Palaios 26, 106–114. http://dx.doi.org/10.2110/palo.2010.p10-097r.

Adachi, N., Nakai, T., Ezaki, Y., Liu, J., 2014. Late Early Cambrian archaeocyath reefs in Hubei Province, South China: modes of construction during their period of demise. Facies 60, 703–717. http://dx.doi.org/10.1007/s10347-013-0376-y.

Aitken, J.D., 1967. Classification and environmental significance of cryptalgal limestones and dolomites, with illustrations from the Cambrian and Ordovician of southwestern Alberta. J. Sediment. Petrol. 37, 1163–1178 DOI: 10.1306/74d7185c-2b21-11d7-8648000102c1865d.

Álvaro, J.J., Debrenne, F., 2010. The Great Atlasian Reef Complex: an early Cambrian sub-tropical fringing belt that bordered West Gondwana. Palaeogeogr. Palaeoclimatol. Palaeoecol. 294, 120–132. http://dx.doi.org/10.1016/j.palaeo.2009.11.022.

Álvaro, J.J., Vennin, E., Moreno-Eiris, E., Perejón, A., Bechstädt, T., 2000. Sedimentary patterns across the Lower–Middle Cambrian transition in the Esla nappe (Cantabrian Mountains, northern Spain). Sediment. Geol. 137, 43–61. http://dx.doi.org/10.1016/S0037-0738(00)00134-2.

Álvaro, J.J., Clausen, S., Albani, A.E., Chellai, E.H., 2006. Facies distribution of the Lower Cambrian cryptic microbial and epibenthic archaeocyathan–microbial communities, western Anti-Atlas, Morocco. Sedimentology 53, 35–53. http://dx.doi.org/10.1111/j.1365-3091.2005.00752.x.

Awramik, S.M., Vanyo, J.P., 1986. Heliotropism in modern stromatolites. Science 231, 1279–1281. http://dx.doi.org/10.1126/science.231.4743.1279.

Bowen, L., Van Vuren, D., 1997. Insular endemic plants lack defenses against herbivores. Conserv. Biol. 11, 1249–1254. http://dx.doi.org/10.1046/j.1523-1739.1997.96368.x.

Bowlin, E.M., Klaus, J.S., Foster, J.S., Andres, M.S., Custals, L., Reid, R.P., 2012. Environmental controls on microbial community cycling in modern marine stromatolites. Sediment. Geol. 263–264, 45–55. http://dx.doi.org/10.1016/j.sedgeo.2011.08.002.

Braga, J.C., Martin, J.M., Riding, R., 1995. Controls on microbial dome fabric development along a carbonate–siliciclastic shelf-basin transect, Miocene, SE Spain. Palaios 10, 347–361. http://dx.doi.org/10.2307/3515160.

Camoin, G.F., Montaggioni, L.F., 1994. High energy coralgal–stromatolite frameworks from Holocene reefs (Tahiti, French Polynesia). Sedimentology 41, 655–676. http://dx.doi.org/10.1111/j.1365-3091.1994.tb01416.x.

Chang, Y., Qi, Y., Zheng, W., Sun, F., 2012. Assemblages and controlling factors of the Cambrian stromatolites in Dengfeng, Henan Province. Acta Micropalaeontologica Sin. 29, 341–351 (in Chinese with English abstract).

Chen, J., Lee, J.-H., 2014. Current progress on the geological record of microbialites and microbial carbonates. Acta Geol. Sin. 88, 260–275. http://dx.doi.org/10.1111/1755-6724.12196.

Chen, J., Chough, S.K., Han, Z., Lee, J.-H., 2011. An extensive erosion surface of a strongly deformed limestone bed in the Gushan and Chaomidian formations (late Middle Cambrian to Furongian), Shandong Province, China: sequence-stratigraphic implications. Sediment. Geol. 233, 129–149. http://dx.doi.org/10.1016/j.sedgeo.2010.11.002.

Chen, J., Chough, S.K., Lee, J.-H., Han, Z., 2012. Sequence-stratigraphic comparison of the upper Cambrian Series 3 to Furongian succession between the Shandong region, China and the Taebaek area, Korea: high variability of bounding surfaces in an epeiric platform. Geosci. J. 16, 357–379. http://dx.doi.org/10.1007/s12303-012-0040-5.

Chough, S.K., Lee, H.S., Woo, J., Chen, J., Choi, D.K., Lee, S.-b, Kang, I., Park, T.-y, Han, Z., 2010. Cambrian stratigraphy of the North China Platform: revisiting principal sections in Shandong Province, China. Geosci. J. 14, 235–268. http://dx.doi.org/10.1007/s12303-010-0029-x.

Connell, J.H., 1978. Diversity in tropical rain forests and coral reefs. Science 199, 1302–1310. http://dx.doi.org/10.1126/science.199.4335.1302.

Debrenne, F., Rozanov, A., 1983. Paleogeographic and stratigraphic distribution of regular archaeocyatha (Lower Cambrian fossils). Geobios 16, 727–736. http://dx.doi.org/10.1016/S0016-6995(83)80089-8.

Elicki, O., 1999. Palaeoecological significance of calcimicrobial communities during ramp evolution: an example from the Lower Cambrian of Germany. Facies 41, 27–40. http://dx.doi.org/10.1007/BF02537458.

England, P.R., Phillips, J., Waring, J.R., Symonds, G., Babcock, R., 2008. Modelling wave-induced disturbance in highly biodiverse marine macroalgal communities: support for the intermediate disturbance hypothesis. Mar. Freshw. Res. 59, 515–520. http://dx.doi.org/10.1071/MF07224.

Ezaki, Y., Liu, J., Adachi, N., 2003. Earliest Triassic microbialite micro- to megastructures in the Huaying Area of Sichuan Province, South China: implications for the nature of oceanic conditions after the End-Permian extinction. Palaios 18, 388–402. http://dx.doi.org/10.1669/0883-1351(2003)018<0388:ETMMTM>2.0.CO;2.

Feng, Q., Gong, Y.-M., Riding, R., 2010. Mid-Late Devonian calcified marine algae and cyanobacteria, south China. J. Paleontol. 84, 569–587. http://dx.doi.org/10.1666/09-108.1.

Flügel, E., 2004. Microfacies of Carbonate Rocks: Analysis. Interpretation and Application. Springer, Berlin (976 pp.).

Gandin, A., Debrenne, F., 2010. Distribution of the archaeocyath–calcimicrobial bioconstructions on the Early Cambrian shelves. Palaeoworld 19, 222–241. http://dx.doi.org/10.1016/j.palwor.2010.09.010.

Gandin, A., Debrenne, F., Debrenne, M., 2007. Anatomy of the Early Cambrian 'La Sentinella' reef complex, Serra Scoris, SW Sardinia, Italy. Geol. Soc. Lond., Spec. Publ. 275, 29–50. http://dx.doi.org/10.1144/GSL.SP.2007.275.01.03.

Garwood, E.J., 1931. The Tuedian Beds of Northern Cumberland and Roxburghshire East of the Liddel Water. Q. J. Geol. Soc. 87, 97–159. http://dx.doi.org/10.1144/gsl.jgs.1931.087.01-04.07.

Geyer, G., Shergold, J., 2000. The quest for internationally recognized divisions of Cambrian time. Episodes 23, 188–195.

Glass, L.M., Phillips, D., 2006. The Kalkarindji continental flood basalt province: a new Cambrian large igneous province in Australia with possible links to faunal extinctions. Geology 34, 461–464. http://dx.doi.org/10.1130/g22122.1.

Hong, J., Cho, S.-H., Choh, S.-J., Woo, J., Lee, D.-J., 2012. Middle Cambrian siliceous sponge–calcimicrobe buildups (Daegi Formation, Korea): metazoan buildup constituents in the aftermath of the Early Cambrian extinction event. Sediment. Geol. 253–254, 47–57. http://dx.doi.org/10.1016/j.sedgeo.2012.01.011.

Hough, M.L., Shields, G.A., Evins, L.Z., Strauss, H., Henderson, R.A., Mackenzie, S., 2006. A major sulphur isotope event at c. 510 Ma: a possible anoxia–extinction–volcanism connection during the Early–Middle Cambrian transition? Terra Nova 18, 257–263. http://dx.doi.org/10.1111/j.1365-3121.2006.00687.x.

Howell, J., Woo, J., Chough, S.K., 2011. Dendroid morphology and growth patterns: 3-D computed tomographic reconstruction. Palaeogeogr. Palaeoclimatol. Palaeoecol. 299, 335–347. http://dx.doi.org/10.1016/j.palaeo.2010.11.013.

Huang, B., Zhu, R., Otofuji, Y.-i, Yang, Z., 2000. The Early Paleozoic paleogeography of the North China block and the other major blocks of China. Chin. Sci. Bull. 45, 1057–1065. http://dx.doi.org/10.1007/BF02887174.

Jahnert, R.J., Collins, L.B., 2011. Significance of subtidal microbial deposits in Shark Bay, Australia. Mar. Geol. 286, 106–111. http://dx.doi.org/10.1016/j.margeo.2011.05.006.

Kah, L.C., Riding, R., 2007. Mesoproterozoic carbon dioxide levels inferred from calcified cyanobacteria. Geology 35, 799–802. http://dx.doi.org/10.1130/g23680a.1.

Kennard, J.M., James, N.P., 1986. Thrombolites and stromatolites: two distinct types of microbial structures. Palaios 1, 492–503. http://dx.doi.org/10.2307/3514631.

Kobluk, D.R., 1985. Biota preserved within cavities in Cambrian *Epiphyton* mounds, upper shady dolomite. J. Paleontol. 59, 1158–1172.

Korde, K.B., 1973. Cambrian Algae. Trudy Paleontologicheskogo instituta, Akademii Nauk SSSR, Moscow (349 pp. (in Russian)).

Kruse, P.D., Zhuravlev, A.Y., 2008. Middle–Late Cambrian *Rankenella–Girvanella* reefs of the Mila Formation, northern Iran. Can. J. Earth Sci. 45, 619–639. http://dx.doi.org/10.1139/e08-016.

Kruse, P.D., Gandin, A., Debrenne, F., Wood, R., 1996. Early Cambrian bioconstructions in the Zavkhan Basin of western Mongolia. Geol. Mag. 133, 429–444. http://dx.doi.org/10.1017/S0016756800007597.

Kwon, Y.K., Chough, S.K., Choi, D.K., Lee, D.J., 2006. Sequence stratigraphy of the Taebaek Group (Cambrian–Ordovician), mideast Korea. Sediment. Geol. 192, 19–55. http://dx.doi.org/10.1016/j.sedgeo.2006.03.024.

Lasemi, Y., Amin-Rasouli, H., 2007. Archaeocyathan buildups within an entirely siliciclastic succession: new discovery in the Toyonian Lalun Formation of northern Iran, the Proto-Paleotethys passive margin of northern Gondwana. Sediment. Geol. 201, 302–320. http://dx.doi.org/10.1016/j.sedgeo.2007.05.015.

Laval, B., Cady, S.L., Pollack, J.C., McKay, C.P., Bird, J.S., Grotzinger, J.P., Ford, D.C., Bohm, H.R., 2000. Modern freshwater microbialite analogues for ancient dendritic reef structures. Nature 407, 626–629. http://dx.doi.org/10.1038/35036579.

Lee, H.S., Chough, S.K., 2011. Depositional processes of the Zhushadong and Mantou formations (Early to Middle Cambrian), Shandong Province, China: roles of archipelago and mixed carbonate–siliciclastic sedimentation on cycle genesis during initial flooding of the North China Platform. Sedimentology 58, 1530–1572. http://dx.doi.org/10.1111/j.1365-3091.2011.01225.x.

Lee, J.-H., Chen, J., Chough, S.K., 2010. Paleoenvironmental implications of an extensive maceriate microbialite bed in the Furongian Chaomidian Formation, Shandong Province, China. Palaeogeogr. Palaeoclimatol. Palaeoecol. 297, 621–632. http://dx.doi.org/10.1016/j.palaeo.2010.09.012.

Lee, J.-H., Chen, J., Chough, S.K., 2012. Demise of an extensive biostromal microbialite in the Furongian (late Cambrian) Chaomidian Formation, Shandong Province, China. Geosci. J. 16, 275–287. http://dx.doi.org/10.1007/s12303-012-0027-2.

Lee, J.-H., Chen, J., Choh, S.-J., Lee, D.-J., Han, Z., Chough, S.K., 2013. Furongian (late Cambrian) sponge–microbial maze-like reefs in the North China Platform. Palaios (in press).

Liu, W., Zhang, X., 2012. *Girvanella*-coated grains from Cambrian oolitic limestone. Facies 58, 779–787. http://dx.doi.org/10.1007/s10347-012-0294-4.

Luchinina, V.A., 2009. *Remalcis* and *Epiphyton* as different stages in the life cycle of calcareous algae. Paleontol. J. 43, 463–468. http://dx.doi.org/10.1134/s0031030109040169.

Mankiewicz, C., 1992. Proterozoic and Early Cambrian calcareous algae. In: Schopf, J.W., Klein, C. (Eds.), The Proterozoic Biosphere: A Multidisciplinary Study. Cambridge University Press, Cambridge, pp. 359–367.

McKenzie, N.R., Hughes, N.C., Myrow, P.M., Choi, D.K., Park, T.-y, 2011. Trilobites and zircons link north China with the eastern Himalaya during the Cambrian. Geology 39, 591–594. http://dx.doi.org/10.1130/g31838.1.

McMenamin, M.A.S., Debrenne, F., Zhuravlev, A.Y., 2000. Early Cambrian Appalachian archaeocyaths: further age constraints from the fauna of New Jersey and Virginia, U.S.A. Geobios 33, 693–708. http://dx.doi.org/10.1016/S0016-6995(00)80123-0.

Meng, X., Ge, M., Tucker, M.E., 1997. Sequence stratigraphy, sea-level changes and depositional systems in the Cambro-Ordovician of the North China carbonate platform. Sediment. Geol. 114, 189–222. http://dx.doi.org/10.1016/s0037-0738(97)00073-0.

Mu, X., Yan, H., Li, Y., Yuan, J., Zhang, J., 2003. Temporal and spatial distribution of microbiolitic reefs of Middle Cambrian, eastern North China Craton. Acta Micropalaeontologica Sin. 20, 279–285 (in Chinese with English abstract).

Park, T.-y, Woo, J., Lee, D.-J., Lee, D.-C., Lee, S.-b, Han, Z., Chough, S.K., Choi, D.K., 2011. A stem-group cnidarian described from the mid-Cambrian of China and its significance for cnidarian evolution. Nat. Commun. 2, 442. http://dx.doi.org/10.1038/ncomms1457.

Peng, S., Babcock, L.E., Zuo, J., Zhu, X., Lin, H., Yang, X., Qi, Y., Bagnoli, G., Wang, L., 2012. Global standard stratotype-section and point (GSSP) for the base of the Jiangshanian Stage (Cambrian: Furongian) at Duibian, Jiangshan, Zhejiang, Southeast China. Episodes 35, 462–477.

Pratt, B.R., 1984. Epiphyton and Renalcis — diagenetic microfossils from calcification of coccoid blue-green algae. J. Sediment. Petrol. 54, 948–971. http://dx.doi.org/10.1306/212f853f-2b24-11d7-8648000102c1865d.

Pratt, B.R., Spincer, B.R., Wood, R.A., Zhuravlev, A.Y., 2001. Ecology and evolution of Cambrian reefs. In: Zhuravlev, A.Y., Riding, R. (Eds.), Ecology of the Cambrian Radiation. Columbia University Press, New York, pp. 254–274.

Read, J.F., Pfeil, R.W., 1983. Fabrics of allochthonous reefal blocks, Shady dolomite (Lower to Middle Cambrian), Virginia Appalachians. J. Sediment. Petrol. 53, 761–778. http://dx.doi.org/10.1306/212F82B5-2B24-11D7-8648000102C1865D.

Rees, M.N., Pratt, B.R., Rowell, A.J., 1989. Early Cambrian reefs, reef complexes, and associated lithofacies of the Shackleton Limestone, Transantarctic Mountains. Sedimentology 36, 341–361. http://dx.doi.org/10.1111/j.1365-3091.1989.tb00611.x.

Riding, R., 1977. Calcified Plectonema (blue-green algae), a recent example of Girvanella from Aldabra Atoll. Palaeontology 20, 33–46.

Riding, R., 1991a. Calcified cyanobacteria. In: Riding, R. (Ed.), Calcareous Algae and Stromatolites. Springer-Verlag, Berlin, pp. 55–87.

Riding, R., 1991b. Classification of microbial carbonates. In: Riding, R. (Ed.), Calcareous Algae and Stromatolites. Springer-Verlag, Berlin, pp. 21–51.

Riding, R., 2000. Microbial carbonates: the geological record of calcified bacterial–algal mats and biofilms. Sedimentology 47, 179–214. http://dx.doi.org/10.1046/j.1365-3091.2000.00003.x.

Riding, R., 2001. Calcified algae and bacteria. In: Zhuravlev, A.Y., Riding, R. (Eds.), Ecology of the Cambrian Radiation. Columbia University Press, New York, pp. 445–473.

Riding, R., Fan, J.S., 2001. Ordovician calcified algae and cyanobacteria, northern Tarim Basin subsurface, China. Palaeontology 44, 783–810. http://dx.doi.org/10.1111/1475-4983.00201.

Riding, R., Tomás, S., 2006. Stromatolite reef crusts, Early Cretaceous, Spain: bacterial origin of in situ-precipitated peloid microspar? Sedimentology 53, 23–34. http://dx.doi.org/10.1111/j.1365-3091.2005.00751.x.

Riding, R., Voronova, L., 1984. Assemblages of calcareous algae near the Precambrian/Cambrian boundary in Siberia and Mongolia. Geol. Mag. 121, 205–210. http://dx.doi.org/10.1017/S0016756800028260.

Riding, R., Voronova, L., 1985. Morphological groups and series in Cambrian calcareous algae. In: Toomey, D.F., Hitecki, M.H. (Eds.), Paleoalgology. Springer, pp. 56–78. http://dx.doi.org/10.1007/978-3-642-70355-3_6.

Rogers, C.S., 1993. Hurricanes and coral reefs: the intermediate disturbance hypothesis revisited. Coral Reefs 12, 127–137. http://dx.doi.org/10.1007/BF00334471.

Rowland, S.M., 1984. Were there framework reefs in the Cambrian? Geology 12, 181–184 http://dx.doi.org/10.1130/0091-7613(1984)12<181:wtfrit>2.0.co;2.

Rowland, S.M., Gangloff, R.A., 1988. Structure and paleoecology of Lower Cambrian reefs. Palaios 3, 111–135. http://dx.doi.org/10.2307/3514525.

Rowland, S.M., Shapiro, R.S., 2002. Reef patterns and environmental influences in the Cambrian and earliest Ordovician. In: Kiessling, W., Flügel, E., Golonka, J. (Eds.), Phanerozoic Reef Patterns. SEPM Special Publication 72, SEPM, Tulsa, pp. 95–128. http://dx.doi.org/10.2110/pec.02.72.0095.

Schluter, D., 2000. The Ecology of Adaptive Radiation. Oxford University, Oxford (296 pp.).

Shapiro, R.S., 2000. A comment on the systematic confusion of thrombolites. Palaios 15, 166–169. http://dx.doi.org/10.1669/0883-1351(2000).

Thomas, D.J., Sullivan, S.L., Price, A.L., Zimmerman, S.M., 2005. Common freshwater cyanobacteria grow in 100% CO_2. Astrobiology 5, 66–74. http://dx.doi.org/10.1089/ast.2005.5.66.

Turner, E.C., Narbonne, G.M., James, N.P., 1993. Neoproterozoic reef microstructures from the Little Dal Group, northwestern Canada. Geology 21, 259–262 http://dx.doi.org/10.1130/0091-7613(1993)021<0259:nrmftl>2.3.co;2.

Woo, J., 2009. The Middle Cambrian Zhangxia Formation, Shandong Province, China: Depositional Environments and Microbial Sedimentation. Ph.D. Thesis Seoul National University, Seoul (243 pp.).

Woo, J., Chough, S.K., 2010. Growth patterns of the Cambrian microbialite: phototropism and speciation of Epiphyton. Sediment. Geol. 229, 1–8. http://dx.doi.org/10.1016/j.sedgeo.2010.05.006.

Woo, J., Chough, S.K., Han, Z., 2008. Chambers of Epiphyton thalli in microbial buildups, Zhangxia Formation (Middle Cambrian), Shandong Province, China. Palaios 23, 55–64. http://dx.doi.org/10.2110/palo.2006.p06-103r.

Wood, R., 1999. Reef Evolution. Oxford University Press, Oxford (414 pp.).

Wood, R., Zhuravlev, A.Y., Anaaz, C.T., 1993. The ecology of Lower Cambrian buildups from Zuune Arts, Mongolia: implications for early metazoan reef evolution. Sedimentology 40, 829–858. http://dx.doi.org/10.1111/j.1365-3091.1993.tb01364.x.

Yang, Z., Otofuji, Y.-i, Sun, Z., Huang, B., 2002. Magnetostratigraphic constraints on the Gondwanan origin of North China: Cambrian/Ordovician boundary results. Geophys. J. Int. 151, 1–10. http://dx.doi.org/10.1046/j.1365-246X.2002.01656.x.

Zhao, X., Coe, R.S., Liu, C., Zhou, Y., 1992. New Cambrian and Ordovician paleomagnetic poles for the North China Block and their paleogeographic implications. J. Geophys. Res. 97, 1767–1788. http://dx.doi.org/10.1029/91JB02742.

Zhuravlev, A.Y., 1986. Evolution of archaeocyaths and palaeobiogeography of the Early Cambrian. Geol. Mag. 123, 377–385. http://dx.doi.org/10.1017/S0016756800033471.

Zhuravlev, A.Y., 1996. Reef ecosystem recovery after the Early Cambrian extinction. In: Hart, M.B. (Ed.), Biotic Recovery from Mass Extinction Events. Geological Society Special Publication, 102. Geological Society, Oxford, pp. 79–96.

Zhuravlev, A.Y., 2001. Biotic diversity and structure during the Neoproterozoic–Ordovician transition. In: Zhuravlev, A.Y., Riding, R. (Eds.), Ecology of the Cambrian Radiation. Columbia University Press, New York, pp. 173–199.

Zhuravlev, A.Y., Wood, R.A., 1996. Anoxia as the cause of the mid-Early Cambrian (Botomian) extinction event. Geology 24, 311–314. http://dx.doi.org/10.1130/0091-7613(1996)024<0311:aatcot>2.3.co;2.